Journal of Air Pollution and Health (Summer 2025); 10(3): 311-328

Original Article

Available online at http://japh.tums.ac.ir

Optimization of window opening, its position and heat source position to obtain maximum air exchange efficiency and heat transfer for a generic cross-ventilated room

Soma Kalia[1], Nibedita Mishra[2], Prakash Ghose[3,*], Vijay Kumar Mishra[3]

[1] Department of Home Science, Ramadevi Women's University, Bhubaneswar, India
[2] Department of Home Science, Puri Women's College, Ramadevi Women's University, Bhubaneswar, India
[3] School of Mechanical Engineering, Kalinga Institute of Industrial Technology (KIIT), Bhubaneswar, India

ARTICLE INFORMATION

Article Chronology:
Received 26 May 2025
Revised 14 June 2025
Accepted 02 August 2025
Published 29 September 2025

Keywords:
Ventilation; Computational fluid dynamics (CFD); Air exchange efficiency; Taguchi; Analysis of variance

CORRESPONDING AUTHOR:
pghosefme@kiit.ac.in
Tel: (+91) 674 274 0326
Fax: (+91) 674 274 0326

ABSTRACT

Introduction: Today, the natural ventilation is emphasized to minimize the energy consumption. It also helps to decrease interior temperatures and maintain internal humidity. In this work, the effect of the rear window opening (factor-1), its position (factor-2) and also the effect of the position of a heat source (factor-3) on Air Exchange Efficiency (AEE) and Heat Source Surface Temperature (HSST) is evaluated.

Materials and methods: The Taguchi Design of Experiment (DOE) is applied to shortlist nine simulations with different combinations of the levels for three factors. Then Computational Fluid Dynamics (CFD) simulations were performed and the responses (AEE & HSST) were recorded. The Signal-to-Noise (S/N) ratio values are evaluated separately for the responses and the rank table is prepared to see the impact of various factors for the best response value. Analysis of Variance (ANOVA) analysis is performed to evaluate the impact percentage of the factors to obtain the best responses.

Results: From the mean S/N plots, the best and the worst combinations of levels of the factors for both responses are identified and then simulated. From the study, it is observed that the rear window opening and the window position has the highest and the lowest impact respectively to obtain the highest AEE. Similarly, the window position and the window opening have almost equal impact on lowering the HSST.

Conclusion: The study concludes that proper positioning of window and its opening can be evaluated to get the best AEE and to transfer the maximum heat from the heat source in the room.

Please cite this article as: Kalia S, Mishra N, Ghose P, Mishra VK. Optimization of window opening, its position and heat source position to obtain maximum air exchange efficiency and heat transfer for a generic cross-ventilated room. Journal of Air Pollution and Health. 2025;10(3): 311-328. https://doi.org/10.18502/japh.v10i3.19593

Introduction

Continuous removal of contaminated room air through fresh air from a space without using any mechanical device is called natural ventilation [1]. Exterior air moves into the room due to the pressure differences between the building and its surroundings. It helps to decrease interior temperatures and maintain internal humidity as well [2]. Natural ventilation supplies fresh air and reduces indoor pollutants including smoke, carbon dioxide, odors, bacteria, dust, and moisture [3, 4]. Natural ventilation offers building occupants fresh air while saving money and using less energy.

An improperly designed building window and its improper positioning affects the natural ventilation. If windows are oversized, a higher surface area allows to move the air in and out across the room. At the same time, it receives more solar radiation energy and makes the room hot if the windows are closed. Similarly, window positioning direction and its configuration also play an important role in effective ventilation. Non-operable windows primarily used as decorative elements and light sources, but cannot used for ventilation. Moreover, they increase the heat due to solar radiation [5]. On the other hand, Operable windows can be opened or closed. Hence, the annual energy consumption in buildings with high occupancy is reduced. Depending on the building's geometry, the surrounding temperature, wind speed, and direction, different amounts of airflow through moveable windows are produced. A well-placed, shaded window on a building can significantly reduce the building's energy use and can have a significant impact on the productivity, and aesthetic comfort of building occupants. In a tropical climate, human thermal comfort is a major issue. The building envelope, or shelter, should operate satisfactorily in terms of regulating heat and light. To accomplish the desired ventilation rate and proper dispersion of fresh air throughout the building, ventilation openings are arranged, located, and controlled to take advantage of the wind and temperature driving forces [6].

Computational Fluid Dynamics (CFD) simulations are widely used to predict the ventilation process and pollutant removal from occupant's domicile [7, 8]. The effect of window-to-wall ratio, orientation and building shape on lighting and thermal comfort in tropical naturally ventilated house is investigated and found that by increasing the value of window to wall ratio, thermal comfort increases by 20-55% whereas electricity consumption for lighting is reduced by 1.5-9.5% only [9]. Several CFD simulations were conducted by varying the window-to-wall ratio for a fixed window size, where the building orientation and shading effects are also considered [10]. Though desired thermal comfort is not achieved by varying the window-to-wall ratio, but with a proper design of windows, 2-6^{o}C of temperature can be reduced with natural ventilation process. The window size and incidence angle of external wind significantly affect the performance of natural ventilation. With an increase in window size, the pressure coefficient increases. The pressure coefficient becomes the highest with 45^{o} incidence angle and lowest with 90^{o} incidence angle of the external wind [11]. In order to enhance the thermal comfort and reduce the CO_2 level, the window design for a naturally ventilated office building is improvised [12]. With the consideration of single-side ventilation, the airflow through the small window (10% window-to-floor ratio) with the half or fully-opened condition is better than large windows. Hence, thermal comfort enhances and CO_2 concentration decreases. Experimentation and CFD simulation are conducted to identify the comfort airflow velocity regions in different shapes of houses (L-shape, Rectangular shape and square shape) with two wall window configurations. Moreover, the effect of airflow velocity on the comfort airflow region has also

been studied [13]. It is observed that with north and south door/window configurations, the highest 26% area inside the house is covered with comfort airflow region. When the school buildings are considered, class rooms are divided by a common corridor. The corridor side windows of a two sided classroom configured buildings are generally in closed position. To make the rooms naturally cross ventilated, a channel is implanted which connect both the rooms [14]. The CFD simulation revealed that the ventilation rate has been increased by 215% in an annual basis with the provision of the channel.

It has been observed that to investigate the ventilation effect, experimentations, as well as CFD works, are performed widely. A large number of different conditions such as window size, window position, window opening, airflow direction, solar radiation, etc. are used for experimentations to identify a proper combination and to get the best ventilating effect. With a minimum number of experimentations, it is possible to identify the effect of the variables on optimum ventilation with the help of the Taguchi design of experiment [15]. Hence, the number of experiments/CFD simulations are reduced and that saves computational time. Analysis of Variance (ANOVA) and Grey Relational Analysis (GRA) are also used to confirm the best conditions to get maximum ventilation. To study the effect of window configuration and furniture arrangement on optimum natural ventilation in an office building, L27 orthogonal array is selected for the design of experiment [16]. It is found that the optimum configuration of window and furniture arrangement enhanced the air charge rate and air exchange efficiency by 0.00293 s^{-1} and 1.09% respectively. The effect of vent position, number and size of the vents on single-side ventilation system are investigated to get the maximum mass flow rate and minimum heat source temperature condition with the help of Taguchi design and ANOVA analysis [17]. It is concluded that the number of vents contributes 60.64% for the best ventilating effect. CFD simulations are performed by following the Taguchi design of experiment to investigate the effect of louver position, heat source position and airflow velocity on ventilation performance [18]. The louver position contribute maximum 5%, whereas airflow velocity has 80% influence to achieve the best ventilating effect.

The Mean Air Age (MAA) is a factor related to air residence time that reveals whether the air all around the room is properly ventilated or not. Air Exchange Efficiency (AEE) is derived from Mean Air Age (MAA). A higher value of AEE indicates that the air flushes out from every corner of the room within less time and vice versa. An air stream with a higher AEE wipes out the pollutants such as CO_2, CO, formaldehyde, volatiles etc., from the house effectively. Hence, the house is continuously exposed to fresh air. As a result, various health issues related to indoor pollutant can be minimized.

The CO_2 tracing method is generally used in experimentation and/or CFD simulation to determine the mean age of air [19]. The gas tracing method for the determination of local mean age of air is used by various researchers [20, 21]. However, in this method, transient simulation has to be performed. On the other hand, a special scalar transport equation is also used to evaluate the mean age of air, where a steady state simulation can evaluate the mean age of air [22]. In this case, the source term of the scalar equation is the density. Air exchange efficiency (AEE) is used as a measure of effective ventilation in several studies [23, 21]. AEE is a derived quantity of MAA. The MAA is determined using CO_2 tracing method experimentally and through CFD simulations. After comparison, it is found that the difference between experimental and simulation results are lies within 10%.

In this work, three types of window openings for the rear window are considered such as;

single slider wall inserted window, double slider window and triple slider window. Also, the position of the window is changed from the reference side wall. The double slider front window is fixed at the middle position of the wall. Hence, in each experiment/simulation, it has a half-opening position. The heat source position is also varied. The contribution of the individual variable on maximum air exchange efficiency (AEE) and minimum HSST is also evaluated. MAA analysis is also conducted in this study. All cases are simulated with the help of Ansys Fluent 19.2 CFD and one case is validated against the in-house experimentation.

Limitation of the work

This investigation provides valuable insights into the effective natural cross-ventilation under different conditions such as, window opening, window positions and heat source positions through AEE. These conditions also significantly affect the cooling of heat source. Hence, in order to investigate the effect of these different conditions on HSST, another study is carried out. This work is carried out under different limitations as well.

First, the wind velocity is considered as 1.11 m/s. This work is conducted keeping on view of the atmospheric condition of tropical city Bhubaneswar. Eleven years' average wind velocity in the tropical city Bhubaneswar is considered in one of our previous research work [13]. From this, it has been observed that the average wind velocity is the highest (around 4.44 m/s) in April and May, whereas, in December and January, the wind velocity is around 1.11 m/s). As 1.11 m/s is the lowest wind velocity around a year, the air circulation rate is also the lowest in this case. As a result, the pollutant removal rate is also affected significantly. Therefore, 3.64 km/hr airflow velocity is considered in this work.

Second, the pollutant dispersion is not considered in this work rather two parameters such as AEE and MAA are considered. AEE is derived from MAA. A higher value of AEE indicates that the air flushes out from every corner of the room within less time and vice versa. An air stream with a higher AEE wipes out the pollutants such as CO_2, CO, formaldehyde, volatiles etc., from the house effectively. Hence, the house is continuously exposed to fresh air. As a result, various health issues related to indoor pollutant can be minimized.

Materials and methods

Physical geometry for the computational modeling

In this work, a generic room is considered with a size of 3.65 x 3.65 x 3.04 m as shown in Fig. 1 a. In order to investigate the cross-ventilation effect, two windows are placed on opposite walls. The door opening is not at all considered. Both frames are sized with a width of 1.82 m 6 and with a height of 1.21 m respectively. To see the effect of window opening on AEE and HSST, three types of windows such as; (i) Single slider wall inserted window (ii) Double slider window and (iii) Triple slider window is used in the rear wall. In the front wall, a Double slider window is used at the middle position of the wall. Half of the front wall is closed, closer to the reference side wall. The window opening on the rear wall is varied by using the single slider, double slider and triple slider wall (1.82, 1.21 and 0.91 m opening). The positions of the rear wall window are also varied by 0.60, 0.91 and 1.21 m from the reference side wall. The rear wall window opening and positions are shown in Fig. 1b.

One heat source of size 0.30 x 0.30 x 0.91 m is placed at 1.82 m from the front wall and its position is varied in the lateral direction that is 0.91, 1.82 and 2.74 m from the side reference wall as shown in Fig. 1 a.

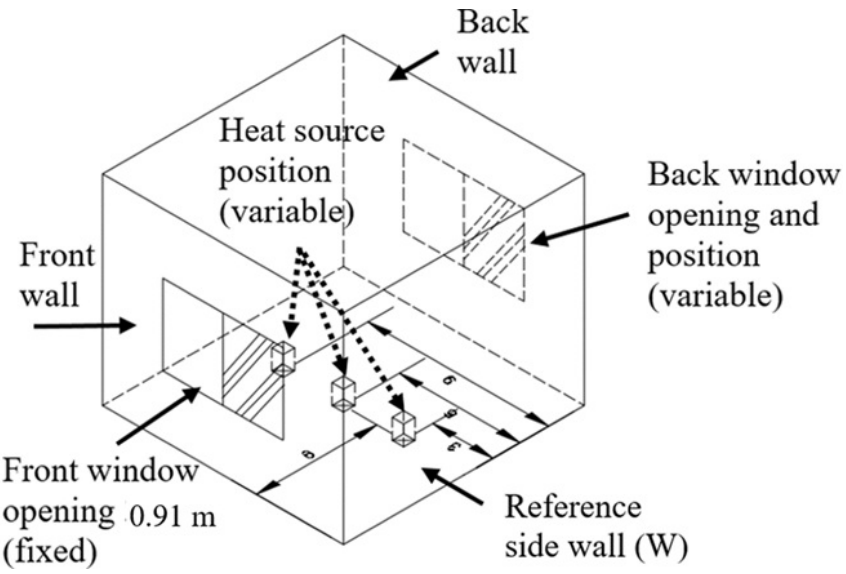

(a)

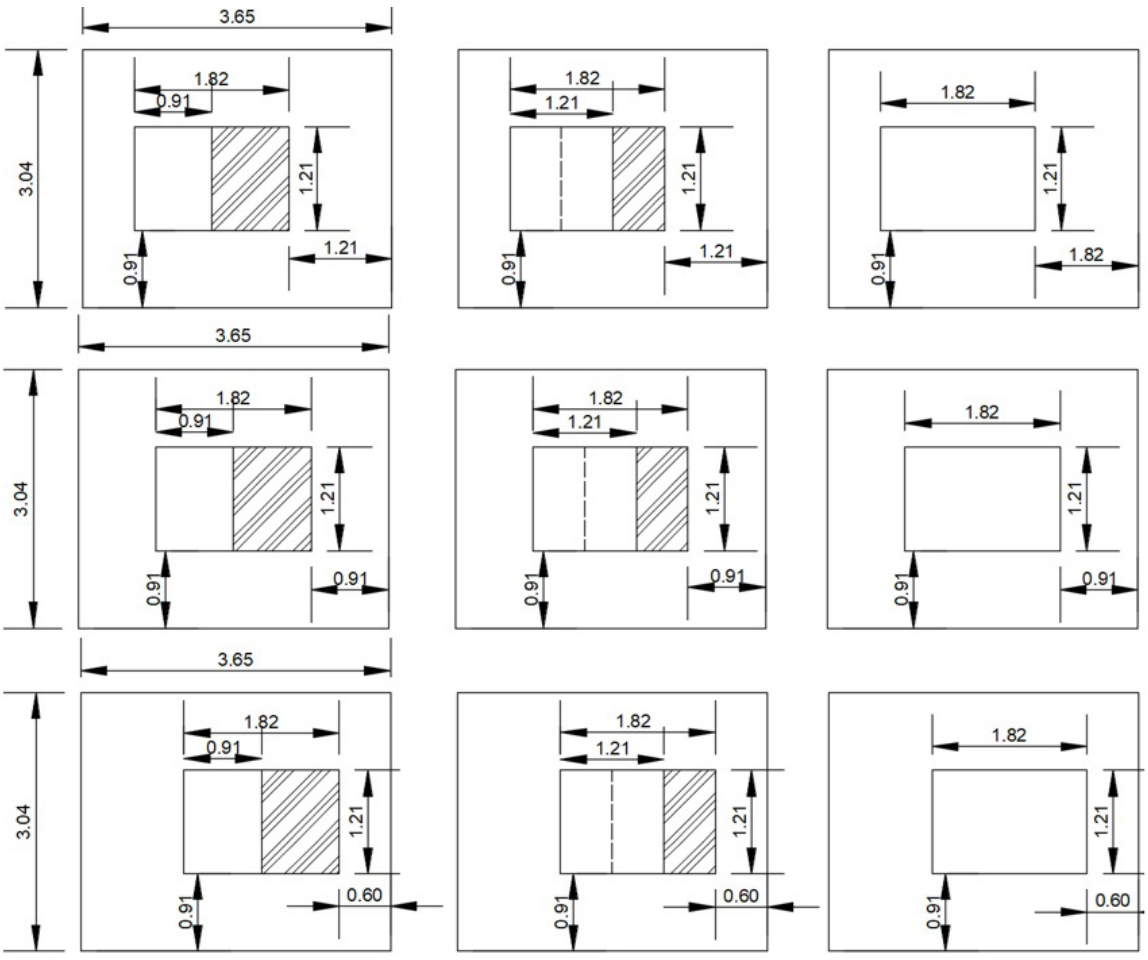

(b)

Fig. 1. (a) Isometric view of the generic cross-ventilated house (b) Various openings and positions of the rear wall window, looking from the front wall (all dimensions are in meter)

Taguchi design of experiment

The Taguchi method encompasses a triad of stages: Design of Experiments (DOE), analysis of Signal-to-Noise (S/N) ratio, and optimization. During the DOE phase, a series of simulations is formulated to explore how different factors impact the process performance. These experiments are structured using orthogonal arrays, which is a systematic arrangement of test cases that efficiently identify the most influential factors. By employing orthogonal arrays, the number of necessary experiments is minimized while ensuring comprehensive testing of all factors across varying levels.

In the S/N ratio analysis phase, each experiment's performance is assessed by gauging the ratio between the desired output (signal) and the undesired output (noise). This S/N ratio aids in identifying the most favourable factor levels that optimize product or process performance. Subsequently, the optimization stage involves deducing the ideal factor levels based on S/N ratio analysis and carrying out validation experiments for confirmation. The S/N ratio is evaluated for two different objectives given as follows [15].

The larger output value is better (AEE)

$$\frac{S}{N} = -10\ log\left(\frac{1}{N}\sum_{i=1}^{N}\frac{1}{Y_i^2}\right) \quad (1)$$

The smaller output value is better (heat source average surface temperature)

$$\frac{S}{N} = -10\ log\left(\frac{1}{N}\sum_{i=1}^{N}Y_i^2\right) \quad (2)$$

In the above equations Y_i is the result of i^{th} objective function. N is the number of repetitions of experiments/simulations. The response table for noise to signal ratio is prepared by averaging the S/N ratio values for the same level presented in DOE table corresponding to its parameter. The delta values of each parameter are evaluated which is the difference between the highest and lowest S/N values for each factor. The largest delta value for a factor shows that the factor is the most effective parameter for the desired output. Then the factors are ranked according to their corresponding delta values. The factor corresponding to the highest delta is given as first rank and the factor corresponding to the lowest delta is given as last rank.

Three parameters such as; (i) rear window opening (A), (ii) rear window position (B) and (iii) heat source position (C) have been considered for this work where the wind velocity is taken as 31.11 m/s. Each parameter varies with three levels. The parameters and their level of variation are illustrated in Table 1. The number of experiments with three parameters and their corresponding level of variation will be evaluated as L^P=27. Therefore, to minimize the number of experiments with a greater extent of accuracy, Taguchi design of experiment is used. The Taguchi DOE is prepared to minimize the number of experiments because each virtual experiment (simulation) takes around 20 h to converge. With the help of Taguchi, L_9 orthogonal array is used where a total of nine experiments are listed with the best combinations of levels of all parameters as shown in Table 2. Minitab software is used to obtain the L_9 array design of experiments.

Table 1. Parameters and their different levels used for simulations

Factors or Parameters (P)	Levels (L)		
	1	2	3
Rear window opening in meter (A)	0.91	1.21	1.82
Rear window position from the side wall, W in meter (B)	0.60	0.91	1.21
Heat source position from the side wall, W in meter (C)	0.91	1.82	2.74

Table 2. Simulation plan of L9 orthogonal array (Taguchi DOE)

Simulation no.	Factors or Parameters		
	A	*B*	*C*
1	1	1	1
2	1	2	2
3	1	3	3
4	2	1	2
5	2	2	3
6	2	3	1
7	3	1	3
8	3	2	1
9	3	3	2

Analysis of Variance (ANOVA)

Analysis of Variance (ANOVA) is used to establish the complex relations between different variables. Here, experimental/computational results are interpreted to obtain the contribution ratio of each factor that affects the desired result. The calculation of ANOVA has been done through the following steps.

The total sum of squares is evaluated as [15];

$$SS_T = \sum_{i=1}^{N}(Y_i - \bar{Y})^2 \quad (3)$$

N is the total number of experiments/simulations listed through Taguchi DOE, Y_i is the result of i^{th} experiment. $\bar{Y}\left(=\frac{1}{N}\sum_{i=1}^{N} Y_i\right)$ is the average value of output results obtained from experiments/ simulations. The sum of the square of one of the parameters or factor P is evaluated as;

$$SS_P = \sum_{j=1}^{t}\frac{(SY_j)^2}{t} - C \quad (4)$$

In the above equation, C is the $\left[\frac{1}{N}\sum_{i=1}^{N} Y_i\right]^2$ the correction factor, j is the level number of that parameter P, t is the number of repetitions of each level of parameter P, SY_j is the sum of the objective result associated with the parameter P and level j. The sum of the square of error is evaluated as;

$$SS_E = SS_T - SS_P \quad (5)$$

In this work, the total degree of freedom and the degree of freedom for each tested parameter are the same as; DF_P=N-1. The contribution ratio percentage (PC) of every parameter and F_P values are evaluated with the help of the following equations [24].

$$PC = \frac{SS_P}{SS_T} \times 100 \quad (6)$$

$$F_P = \frac{V_P}{V_{error}} \quad (7)$$

$$V_{error} = \frac{SS_E}{DF_P} \quad (8)$$

$$V_P = \frac{SS_P}{DF_P} \quad (9)$$

Computational modeling

In this problem, airflow occurs across the windows along with heat transfer from the heat source placed in the interior environment. The heat transfer from the heat source occurs due to airflow around the body by the inlet air (force convection) as well as due to the density variation

of air closer to the heat source body surface (natural convection). Moreover, the flow is turbulent in nature. Therefore, the time-averaged conservation of mass and momentum and energy equations are solved using Ansys-Fluent 19.2 software to obtain the pressure and velocity field in the computational domain. In order to incorporate the buoyancy effect, a source term is used in the Y-momentum equation as; $S_m=\rho g\beta(T-T_\infty)$, where the term β is the thermal expansion coefficient. β is evaluated as the inverse of the sum of wall and room air temperature in Kelvin. ρ is the standard density of air. T and T_∞ are the temperature over the hot source surface and room temperature respectively. The heat source S_e is a constant that continuously generates heat in terms of watts per unit volume. To evaluate the additional terms that have been formed after the time averaging of instantaneous governing equations, the Boussinesq equation and different turbulent flux equations are solved iteratively. The governing equations are given as follows;

Conservation of mass

$$\frac{\partial}{\partial x_i}(\rho\bar{u}_i)=0 \quad (10)$$

Conservation of momentum

$$\frac{\partial}{\partial x_i}\left(\rho\bar{u}_i\bar{u}_j\right)=-\frac{\partial\bar{p}}{\partial x_i}+\frac{\partial}{\partial x_j}\left(\bar{\tau}_{ij}-\rho\overline{u_i'u_j'}\right)+S_m \quad (11)$$

Conservation of energy

$$\frac{\partial}{\partial x_i}\left(\rho\bar{u}_j\bar{h}\right)=\frac{\partial}{\partial x_i}\left(\Gamma_h\frac{\partial\bar{h}}{\partial x_i}-\rho\overline{h''u_j''}\right)+S_e \quad (12)$$

Conservation of local mean age of air (MAA) equation [22]

$$\frac{\partial}{\partial x_i}\left(\rho\bar{u}_j\bar{\phi}\right)=\frac{\partial}{\partial x_i}\left(\Gamma_\phi\frac{\partial\bar{\phi}}{\partial x_i}-\rho\overline{\phi''u_j''}\right)+S_\phi \quad (13)$$

An additional scalar equation is solved using the user-defined scalar (UDS) option in Ansys-Fluent, where, ϕ is the mean age of air scalar variable, the diffusion coefficient of mean age of air scalar; $\Gamma_\phi=\rho D+\frac{\mu_t}{Sc_t}$ .The mass diffusivity $D=2.88\times10^{-8}$, turbulent Schmidt number $Sc_t=0.7$. S_ϕ is the source term, which is nothing but density in the MAA conservation equation. In the convective term of the scalar conservation equation in Ansys-Fluent, the density is multiplied by the scalar variable ϕ. Therefore, to nullify the density, the density is used as the source term. Hence, the equation form becomes $\frac{D(\rho\phi)}{Dt}=\rho$. Now, the equation becomes $D\phi=Dt$. It does mean that the scalar variable ϕ (local mean age of air) is nothing but the air residence time. In order to evaluate the diffusivity and source term, UDFs (User Defined Functions) are used in the UDS (User Defined Scalars) equation. To evaluate the eddy viscosity required to solve the Boussinesq, the standard form of k and ε equations are solved given as follows.

$$\frac{\partial}{\partial x_i}(\rho k\bar{u}_i)=\frac{\partial}{\partial x_j}\left[\left(\mu+\frac{\mu_t}{\sigma_k}\right)\frac{\partial k}{\partial x_j}\right]+G_k+\rho\varepsilon \quad (14)$$

$$\frac{\partial}{\partial x_i}(\rho\varepsilon\bar{u}_i)=\frac{\partial}{\partial x_j}\left[\left(\mu+\frac{\mu_t}{\sigma_\varepsilon}\right)\frac{\partial\varepsilon}{\partial x_j}\right]+C_{1\varepsilon}\frac{\varepsilon}{k}G_k-C_{2\varepsilon}\rho\frac{\varepsilon^2}{k} \quad (15)$$

The term, Gk is values as,

$$G_k=\left(\mu_t\left(\frac{\partial\bar{u}_i}{\partial x_j}+\frac{\partial\bar{u}_j}{\partial x_i}\right)-\frac{2}{3}\rho k\delta_{ij}\right)\frac{\partial\bar{u}_j}{\partial x_i} \quad (16)$$

Turbulent viscosity is obtained from the dimensional analysis as; $\mu_t=C\rho\rho vl=C_\mu\rho\frac{k^2}{\varepsilon}$, where C_μ a model constant and its value is taken as 0.09. $v=k^{1/2}, l=\frac{k^{3/2}}{\varepsilon}$, where v is the velocity scale and l is the length scale. $C_{1\varepsilon}$, $C_{2\varepsilon}$, σ_k (turbulent Prandtl number for k) and σ_ε (turbulent Prandtl number for ε) in the k and ε equations are the model constants. Standard values of them is used for the simulation.

Boundary conditions for CFD modeling

The front wall window opening is the velocity

inlet boundary where the inlet velocity is set as 1.11 m/s for every case. The rear wall window opening is the pressure outlet boundary and the heat source body generates heat of 10000 W/m^3. The floor, roof and all four walls along with the closed portion of the windows are treated as no-slip walls.

A SIMPLE algorithm is used for the pressure-velocity coupling. The second-order upwind scheme is used for spatial discretization. The convergence criteria for all the governing equations are set as 10^{-3}, whereas the convergence criteria for the energy equation is set as 10^{-6}.

Calculation of air exchange efficiency (AEE)

The air exchange efficiency is a parameter that indicates the effective ventilation in a building. In order to evaluate the AEE, the MAA distribution field is first evaluated with the help of the governing Eq. 13. AEE is expressed mathematically as [16];

$$AEE = \frac{\tau_n}{2\bar{\tau}} \times 100 \quad (17)$$

Where, τ_n is the area-weighted average of MAA at the outlet window and $\bar{\tau}$ is the volume average of MAA inside the room. The higher value of τ_n signify that the time taken by the inlet air to reach the outlet boundary is high. That means, as the value of τ_n increases, the air is properly circulated through the room. Similarly, a smaller value of $\bar{\tau}$ means that the air residence time inside the house is small. Therefore, the higher AEE signifies that the air flushes out from every corner of the room within less time and vice versa.

Results and discussion

Experimental validation

In order to evaluate the proficiency of computational modeling, experimental validation has been performed. In this validation process, experimentation on the actual size house (3.65 × 3.65 × 3.04 m) has not been conducted because of its large size that cannot be placed inside the wind tunnel test section. Moreover, it will be expensive to prepare this large real size house. Therefore, a scaled model is prepared for the experimentation at a scale ratio 1:24. Hence, the scale model dimension is 0.152 × 0.152 × 0.127 m. The scale model window opening, its position and the heat source position is kept according to the test number 9 mentioned in Table 2. In test number 9, the factors A, B and C are at the level of 3, 3 and 2 respectively. It means that the factor A (Rear window opening in m) is 6', the factor B (Rear window position from the side wall, W in m) is 1.82 m and the factor C (Heat source position from the side wall, W) is 1.82 m. Similarly, another 3D CAD (3 Dimensional Computer Added Design) scaled model is prepared with a same dimension as the experimental model. The levels of the factors A, B and C are also kept same as the experimental model. However, for validation purposes, only the flow is considered without any heating of the heat source for the validation work.

The Reynolds number $\left(Re = \frac{\rho V_{act} D_{h_{act}}}{\mu}\right)$ is evaluated using the actual inlet velocity (V=1.11 m/s). The hydraulic diameter used for evaluating the Reynolds number is calculated as; D_h=4A/P. Where, A and P are the cross-sectional areas of the front wall window opening and front wall opening perimeter respectively of the actual size house. In the mentioned equations, ρ and μ are the density and viscosity of air at STP (standard temperature and pressure condition) respectively. Then the inlet velocity of air for the scaled model is evaluated using the evaluated Reynolds number $\left(V_{model} = \frac{\mu . Re}{\rho D_{h_{model}}}\right)$.

The 3D CAD scaled model is discretized with 0.8 million cells. This optimum mesh size is preferred from the grid independence test. The inlet airflow velocity evaluated from the Reynolds number as 25.22 m/s and which is used in the scaled model simulation.

The scaled model is shown in Fig. 2a. The experiment is conducted using a subsonic

wind tunnel as shown in Fig. 2b. The inlet airflow velocity is adjusted to 25.22 m/s by adjusting the fan speed of the wind tunnel. The airflow velocity is measured using a hot wire anemometer.

The velocity distribution is measured along the line drawn at the mid-horizontal plane as shown in Fig. 3a. Fig. 3b depicts the comparison of the measured and the CFD result. It shows that throughout the length, the simulated results are pretty close to the experimental results. The maximum and minimum deviation of computational result from the experimental output is 4.55% and 1.33% respectively.

(a) (b)

Fig. 2. (a) Scaled model (1:24) for experimentation (b) Wind tunnel experimental

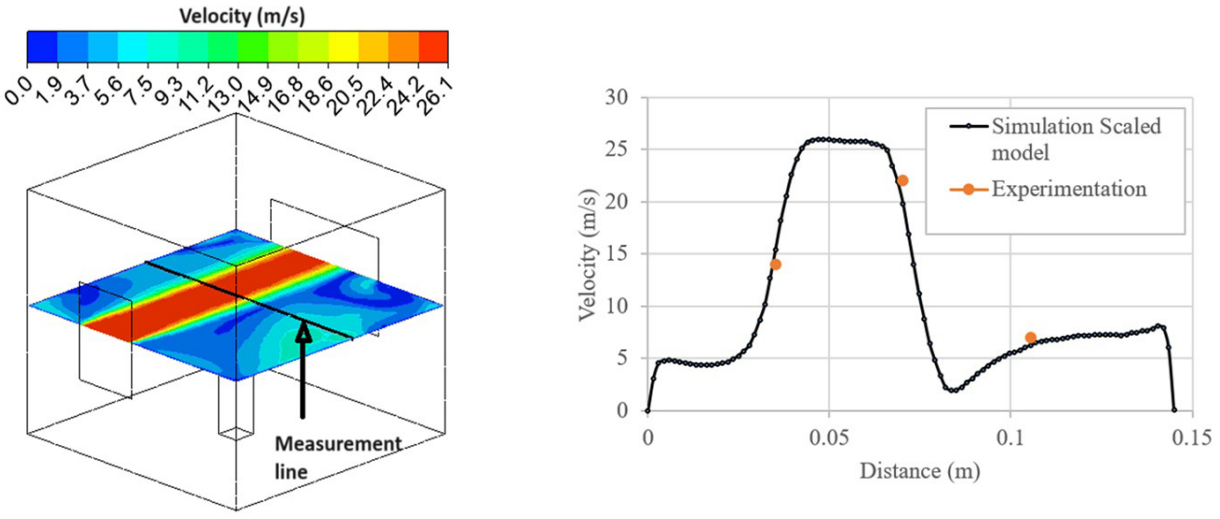

(a) (b)

Fig. 3. (a)Velocity field on the mid-plane of the scaled model (b) Velocity distribution along the measurement line of the scaled model

The resulting data obtained from various simulations is given in Table 3. The airflow velocity for each case is kept constant at 1.11 m/s The air charge rate is also given in Table 3 which is evaluated as; $= \frac{Air\ discharge\ rate}{Volume\ of\ the\ room}$. The discharge rate is the product of the cross-sectional area of the inlet window and inlet airflow velocity. The main objective of the study is to obtain the minimum surface temperature of the hot source surface and to get the maximum AEE. For the HSST, simulation no-3 has the best combination of levels with factors among the all simulations listed in Table 3. Similarly, for AEE, simulation no. 7 has the best combination of levels with factor among the all simulations listed in Table 3. Simulations 7&8 give the lowest (best) and the highest (worst) MAA inside the room respectively. However, the best and worst combination of levels with the factors may or may not be designed by Taguchi DOE. Therefore, mean S/N ratio plots are prepared in the following sections to evaluate the best and the worst combinations of the levels with factors.

Table 3. Main response table, S/N ratio on each simulation for the AEE & HSST

Simulation No.	Factors or Parameters			Air charge rate (ACR) (s^{-1})	Maximum local mean air age (MAA) (s)	Area weighted average surface temperature of the heat source (K)	Air exchange efficiency (AEE) in percentage	S/N AEE	S/N Heat source surface temperature (HSST)
	A	*B*	*C*						
1	1	1	1		130.49	455.32	25.62	28.1716	-53.1663
2	1	2	2		117.57	442.50	26.25	28.3826	-52.9183
3	1	3	3		122.43	421.13	28.27	29.0265	-52.4883
4	2	1	2		93.69	435.57	35.39	30.9776	-52.7812
5	2	2	3	0.0303	115.22	433.44	31.12	29.8607	-52.7386
6	2	3	1		141.35	442.92	32.20	30.1571	-52.9265
7	3	1	3		83.19	442.91	46.63	33.3733	-52.9263
8	3	2	1		154.43	474.47	34.12	30.6602	-53.5242
9	3	3	2		146.85	462.59	33.10	30.3965	-53.3039

Optimization of the factor and levels to obtain the highest AEE and lowest HSST

The S/N ratio for the AEE and HSST are evaluated and listed in Table 3 for all nine simulations. Table 4 shows the average of the S/N ratios of the same levels corresponding to their factors for the both responses (AEE and HSST). Mean effect plots of the S/N ratios for both AEE and HSST are plotted as shown in Figs. 4a & 4b.

For the highest value of AEE, the highest values of S/N ratios from each factor are considered. Hence, A_3-B_1-C_3 (level-3 of parameter A, window opening, level-1 of parameter B, i.e. Rear window position is 0.60 m from the reference wall, level-3 of parameter C, i.e. heat source position is 2.74 m from the reference wall) combination is found as the best for the highest AEE and which is listed in the DOE table (Table 2 & Table 3) as simulation no-7. Similarly, for the lowest value of AEE, the lowest values of S/N ratios from each factor are considered. Hence, corresponding to the lowest values of the S/N ratio, A_1-B_2-C_1 gives the lowest AEE (worst condition for AEE) which is not listed in the table. Therefore, an additional simulation is conducted for the worst condition of AEE and explained in the following sections.

For the lowest value of HSST, the lowest values of S/N ratios from each factor are considered. Hence, for the lowest HSST, A_2-B_3-C_3 combination is found as the best which is not listed in the DOE table (Table 2 & Table 3). Therefore, an additional simulation is conducted for the best condition of HSST which is explained in the following sections. Similarly, for the highest value of HSST, the highest values of S/N ratios from each factor are considered. Hence, corresponding to the highest values of the S/N ratio, A_3-B_2-C_1 gives the highest HSST (worst condition for HSST) which is listed in the DOE table (Table 2) as simulation no-8.

Table 4. Response for Signal to Noise Ratios for the AEE (Larger is better) and HSST (Smaller is better)

	For AEE			For Surface heat source surface temperature (HSST)		
Level	A	B	C	A	B	C
1	29.10	29.76	29.44	-52.86	-52.96	-53.21
2	29.64	29.43	29.51	-52.82	-53.06	-53.00
3	29.95	29.50	29.74	-53.25	-52.91	-52.72
Delta	0.85	0.33	0.30	0.44	0.15	0.49
Rank	1	2	3	2	3	1

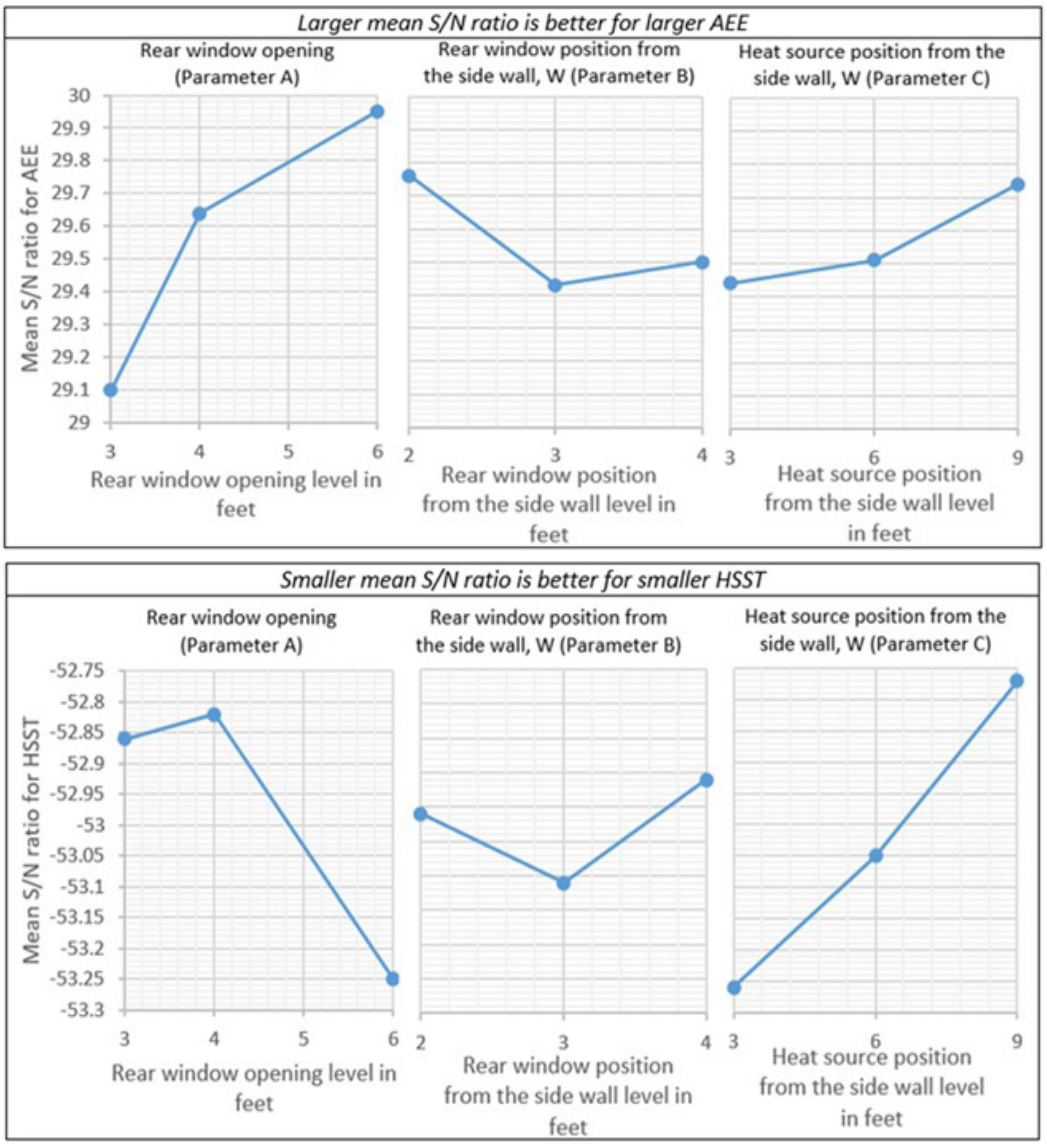

Fig. 4. Effect of rear window opening (A), rear window position (B) and heat source position on (a) Air exchange efficiency (AEE) (b) Heat source surface temperature (HSST)

The influence of the factors A,B and C on AEE and HSST can be determined on the basis of delta value mentioned in Table 4. Corresponding to the AEE rank table, the factor having the highest delta value has the maximum influence to get the better AEE and corresponding to the HSST rank table, the factor having the highest delta value has the maximum influence to get the low HSST. Hence, from Table 4, it is observed that the effect of window opening has the highest impact and the heat source position has the lowest impact on AEE. Similarly, from Table 4, it is also observed the heat source position has the highest impact and the window position has the lowest impact on HSST.

From the ANOVA analysis shown in Table 5, it is also confirmed that the effect of window opening has the highest and the heat source position has the lowest impact on AEE. Around 82.14% contribution of rear window opening (A), 6.25% contribution of rear window position (B) and 3.85 % contribution of the heat source position (C) has been observed for better AEE.

The ANOVA also confirmed that the effect of the heat source position has the highest and the window position has the lowest impact on HSST. Around 45.05% contribution of rear window opening (A), 4.81% contribution of window position (B) and 45.17% contribution of heat source position (C) to obtain a low HSST.

Table 5. ANOVA table for the percentage contribution of each factor on maximization of AEE and minimization of HSST

Parameter		For AEE				For HSST			
		Seq SS	Adj SS	Adj MS	Contribution	Seq SS	Adj SS	Adj MS	Contribution
A	2	208.02	208.02	104.01	82.14%	759155663	759155663	379577832	45.08%
B	2	9.739	9.739	4.869	6.25%	80922217	80922217	40461108	4.81%
C	2	15.833	15.833	7.917	3.85%	757755512	757755512	378877756	45.17%
Error	2	19.667	19.667	9.834	7.77%	82963219	82963219	41481609	4.94%
Total	8	253.26			100%	1680796611			100%

From the mean effect S/N ratio plots, the best combinations of the levels of various factors are already evaluated for the highest AEE and highest HSST. However, from the S/N plot, it is found that the level-factor combination for the lowest AEE and lowest HSST are not listed in the DOE table (Table 2). Therefore, additional simulations are performed for those cases. Table 6 shows that the A_3-B_1-C_3 level-factor combination gives the best AEE as 46.63%. Similarly, A_1-B_3-C_1 level-factor combination gives the worst AEE as 23.51%.

Table 6 also shows that A_2-B_3-C_3 level-factor combination gives the best HSST as 418.97 K. Similarly, A_1-B_3-C_1 level-factor combination gives the worst HSST as 474.47 K.

MAA distribution and surface temperature distribution for the optimum cases

Fig. 4a shows the local MAA distribution at different horizontal planes for different cases. A higher value of MAA in a particular region indicates the higher residence time of the air in that region. Therefore, a higher value of MAA generally leads to a lower AEE which can be observed from Fig. 5. However, a higher value of the average MAA at the outlet window also leads to a higher AEE. A higher value of the average MAA at the outlet indicates that the air inside the room is properly circulated throughout and finally reaches to the outlet boundary. As a result, it takes a longer time to reach the outlet. Therefore, although the highest value of MAA is 154.43 s for case-8, the AEE is 32.13% due to the lower MAA value at the outlet for this case. On the other hand, the highest AEE is observed as 46.63% for case-7 but the highest MAA for this simulation is less than case-8. It happens due to the higher MAA at the outlet boundary for case-8.

Table 6. Verification table

Higher is better		Lower is better	
AEE for the best case (A_3-B_1-C_3), listed in Table 4 (Simulation no.-7)	AEE for the worst case (A_1-B_2-C_1), not listed in Table 4	Average surface temperature (K) of heat source best case (A_2-B_3-$C_{3)}$, not listed in Table 4	Average Surface temperature (K) of heat source worst case (A_3-B_2-$C_{3)}$, listed in Table 4 (Simulation no.-8)
46.63%	23.51%	418.97	474.47

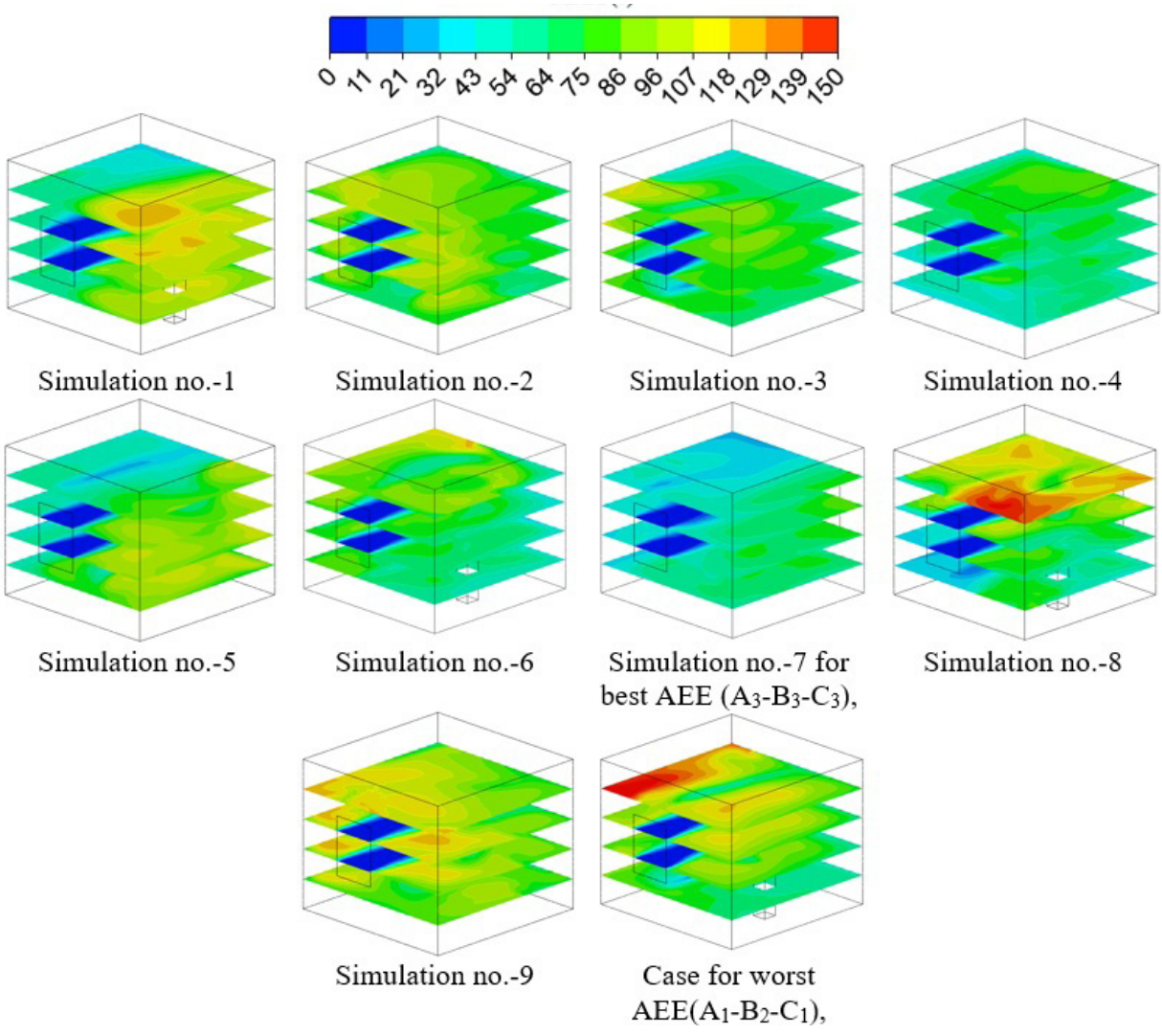

Fig. 5. Local MAA for various cases

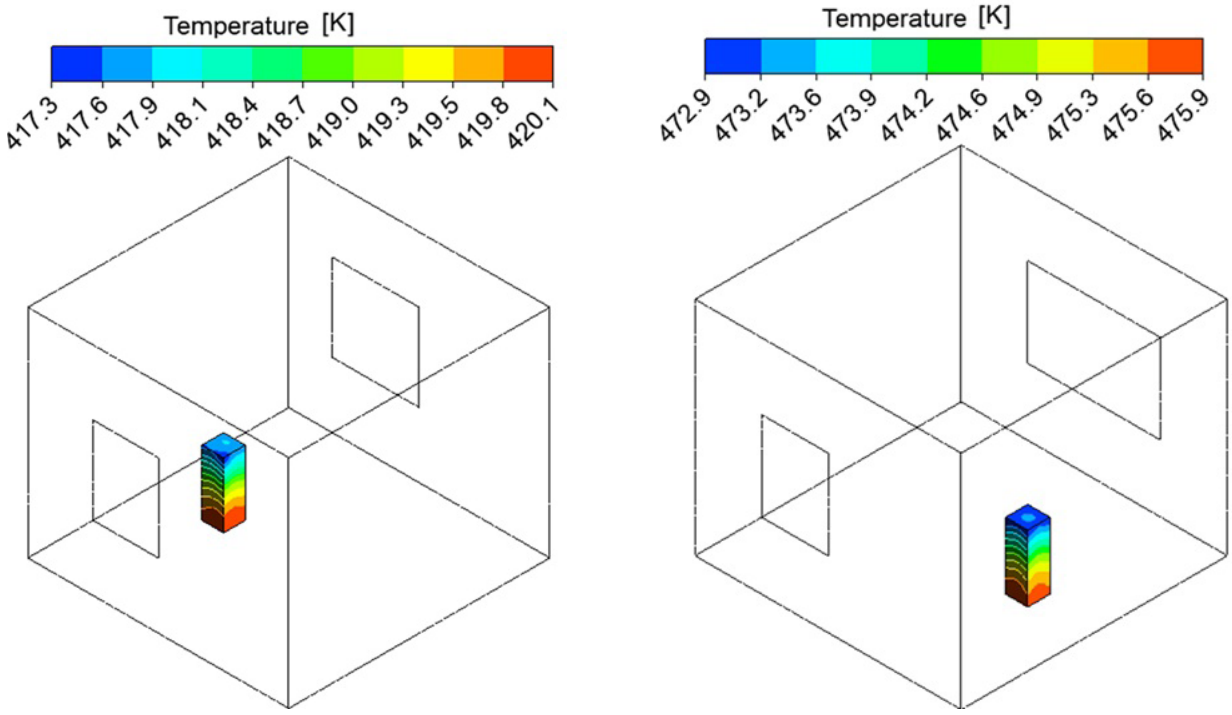

(a) (b)

Fig. 6. Surface temperature distribution of heat source for the case (a) A_2-B_3-C_3 (best case) [A_2-B_3-C_3 (level-3 of parameter A, i.e. 1.21 m window opening, level-1 of parameter B, i.e. rear window position is 1.21 m from the reference wall, level-3 of parameter C, i.e. heat source position is 2.74 m from the reference wall)] (b) case A_3-B_2-C_1 (worst case) [A_3-B_2-C_1 (level-3 of parameter A, i.e. 1.82 m window opening, level-1 of parameter B, i.e. rear window position is 0.91 m from the reference wall, level-3 of parameter C, i.e. heat source position is 0.91 m from the reference wall)]

Fig. 6a, b shows the temperature distribution over the surface of the heat source. However, different scales for both the best (A_2-B_3-C_3) and the worst (A_3-B_2-C_1) cases are selected for the proper visualization. From the scale of the figures, it can be observed that the maximum and minimum temperatures for the best case is 417 K to 421 K respectively. Similarly, the maximum and the minimum range of temperature for the worst case is 472 K to 476 K respectively.

Conclusion

To evaluate the effect of the rear window opening, the rear window position and the position of the heat source inside the room on AEE and HSST, various simulations are conducted for a generic room of size 3.65 × 3.65 × 3.04 m. The inlet airflow velocity is maintained as 1.11 m/s for every case. The computational model is validated against the experimental result of a scaled model. Using the Taguchi DOE, the total simulations are reduced to nine. The computational results (responses) such as; AEE and HSST for each case are recorded. From the Taguchi, every factor is ranked according to their influence on the responses. The rank is verified with the help of ANOVA and the percentage contribution of every factor on the responses is also evaluated through ANOVA. From the S/N ratio mean effect plot, the best and the worst combination of the levels are identified and the corresponding simulations are performed. Then the S/N ratio mean effect plot's

suggestion is verified.

From the work, it is observed that the effect of the rear window opening has the highest (82.14%) impact and the window position has the lowest impact (3.85%) on AEE (for a higher AEE). Similarly, the heat source position has the highest impact (45.17%) and the rear window position has the lowest impact (4.81%) impact on HSST (for a lower surface temperature).

The best and the worst combination of levels with the factors for the best AEE is identified as A_3-B_1-C_3 and A_1-B_2-C_1 respectively. For the best and the worst cases, the AEE is determined as 46.63% and 23.51% respectively.

The best and the worst combination of the levels with the factors for lowering the HSST is identified as A_2-B_3-C_3 and A_3-B_2-C_1 respectively. For the best and the worst cases, the HSST is identified as 418.97 K and 474.47 K respectively.

Future work direction

The present study gives a basic understanding of how the rear window opening, window position, and heat source location influence Air Exchange Efficiency (AEE) and Heat Source Surface Temperature (HSST) in a generic room. However, this work can be extended by including various aspects given as follows:

All the simulations are conducted with steady state airflow condition. The work can be extended to evaluate the effect of transient effect such as wind jerk condition, dynamic occupancy and time dependent environmental conditions. Inlet airflow direction, multi directional window configuration, multiple heat sources and furniture positioning effect within commercial and residential buildings may be considered to understand the real world scenario. Effect of different window design and room design can also be analysed. Moreover, the latest optimization technology can be used to evaluate the optimum AEE and HSST conditions. Last but not the least, the dispersion of various pollutants like CO_2, CO, formaldehyde, volatile matters and particulate matters inside the room and their removal efficiency with different inlet condition can be analysed.

Financial supports

No funding was received from any financial organization to conduct this research.

Competing interests

The authors declare that they have no known financial or non-financial competing interests in any material discussed in this paper.

Acknowledgements

We would like to express our sincere gratitude to Head of the Aerospace engineering department of KIIT Deemed to be University for supporting the experiment conducted in wind tunnel.

Ethical considerations

"Ethical issues (Including plagiarism, Informed Consent, misconduct, data fabrication and/or falsification, double publication and/or submission, redundancy, etc.) have been completely observed by the authors.

References

1. Yin W, Zhang G, Yang W, Wang X. Natural ventilation potential model considering solution multiplicity, window opening percentage, air velocity and humidity in China. J Building Environment. 2010;45(2):338-44.

2. Costanzo V, Yao R, Xu T, Xiong J, Zhang Q, Li B. Natural ventilation potential for residential buildings in a densely built-up and highly polluted environment. A case study. J Renewable Energy. 2019;138:340-53.

3. Escombe AR, Oeser CC, Gilman RH, Navincopa M, Ticona E, Pan W, et al. Natural ventilation for the prevention of airborne contagion. J PLoS medicine. 2007;4(2):e68.

4. Kalia S, Mishra N, Ghose P. Indoor air quality assessment of an existing apartment located in Indian tropical city, Bhubaneswar. J Journal of Air Pollution Health. 2024.

5. Zhai ZJ, Johnson M-H, Krarti M.

Assessment of natural and hybrid ventilation models in whole-building energy simulations. J Energy Buildings. 2011;43(9):2251-61.

6. Szokolay S, Koenigsberger O. Manual of tropical housing and building. 1973.

7. Xie H, Zhang TJJoAP, Health. Impact of roof shape on indoor gaseous pollutant level for natural ventilation buildings in a street canyon: Numerical simulation. 2023;8(3):339-60.

8. Wu J, Long F, Deng B, Health. Numerical simulation of VOCs emission from building materials: A comparison of different material shapes. J Journal of Air Pollution Health. 2022;7(2):109-20.

9. Pathirana S, Rodrigo A, Halwatura R. Effect of building shape, orientation, window to wall ratios and zones on energy efficiency and thermal comfort of naturally ventilated houses in tropical climate. J International Journal of Energy Environmental Engineering. 2019;10(1):107-20.

10. Aldawoud A. Windows design for maximum cross-ventilation in buildings. J Advances in building energy research. 2017;11(1):67-86.

11. Sacht H, Lukiantchuki MA. Windows size and the performance of natural ventilation. J Procedia Engineering. 2017;196:972-9.

12. Abdullah HK, Alibaba HZ. Window design of naturally ventilated offices in the mediterranean climate in terms of CO_2 and thermal comfort performance. J Sustainability. 2020;12(2):473.

13. Kalia S, Mishra N, Ghose P. Impact of Internal Wall Barriers on Airflow Pattern in Natural Cross-Ventilation of the Common Houses in Bhubaneswar City, India. J Jordan Journal of Mechanical Industrial Engineering. 2023;17(1).

14. Zhang Z-Y, Yin W, Wang T-W, O'Donovan A. Effect of cross-ventilation channel in classrooms with interior corridor estimated by computational fluid dynamics. J Indoor Built Environment. 2022;31(4):1047-65.

15. Yuce BE, Nielsen PV, Wargocki P. The use of Taguchi, ANOVA, and GRA methods to optimize CFD analyses of ventilation performance in buildings. J Building Environment. 2022;225:109587.

16. Yin X, Muhieldeen MW, Razman R, Ee JYC. Multi-objective optimization of window configuration and furniture arrangement for the natural ventilation of office buildings using Taguchi-based grey relational analysis. J Energy Buildings. 2023;296:113385.

17. Lenin V, Sivalakshmi S, Raja M. Optimization of window type and vent parameters on single-sided natural ventilation buildings. J Journal of Thermal Analysis Calorimetry. 2019;136(1):367-79.

18. Chandra AS, Reddy PN, Harish R. Natural ventilation in a lege space with heat source: CFD visualization and taguchi optimization. J Journal of Thermal Engineering. 2022;8(5):642-55.

19. Buratti C, Mariani R, Moretti E. Mean age of air in a naturally ventilated office: Experimental data and simulations. J Energy Buildings. 2011;43(8):2021-7.

20. Hang J, Sandberg M, Li Y. Age of air and air exchange efficiency in idealized city models. J Building Environment. 2009;44(8):1714-23.

21. Hormigos-Jimenez S, Padilla-Marcos MA, Meiss A, Gonzalez-Lezcano RA, Feijó-MuÑoz J. Experimental validation of the age-of-the-air CFD analysis: A case study. J Science Technology for the Built Environment. 2018;24(9):994-1003.

22. Ning M, Mengjie S, Mingyin C, Dongmei P, Shiming D. Computational fluid dynamics (CFD) modelling of air flow field, mean age of air and CO_2 distributions inside a bedroom with different heights of conditioned air supply outlet. J Applied energy. 2016;164:906-15.

23. Yazarlou T, Barzkar E. Louver and window position effect on cross-ventilation in a generic isolated building: A CFD approach. J Indoor Built Environment. 2022;31(6):1511-29.

24. Bademlioglu A, Canbolat A, Yamankaradeniz N, Kaynakli O. Investigation of parameters affecting Organic Rankine Cycle efficiency by using Taguchi and ANOVA methods. J Applied Thermal Engineering. 2018;145:221-8.